ADVANCED MATERIALS

Supporting Information

for *Adv. Mater.*, DOI: 10.1002/adma.201803220

The Marriage of the FeN_4 Moiety and MXene Boosts Oxygen Reduction Catalysis: Fe 3d Electron Delocalization Matters

Zilan Li, Zechao Zhuang, Fan Lv, Han Zhu, Liang Zhou, Mingchuan Luo, Jiexin Zhu, Zhiquan Lang, Shihao Feng, Wei Chen, Liqiang Mai,* and Shaojun Guo**

Supporting Information

for *Adv. Mater.*, DOI: 10.1002/adma.201803220

The Marriage of FeN_4 Moiety and MXene Boosts Oxygen Reduction Catalysis: Fe 3*d* Electron Delocalization Matters

Zilan Li, Zechao Zhuang, Han Zhu, Fan Lv, Liang Zhou, Mingchuan Luo, Jiexin Zhu, Ziquan Lang, Shihao Feng, Wei Chen, Liqiang Mai,* and Shaojun Guo**

Z. Li,[+] Z. Zhuang,[+] Prof. L. Zhou, J. Zhu, Z. Lang, S. Feng, Prof. W. Chen, Prof. L. Mai

State Key Laboratory of Advanced Technology for Materials Synthesis and Processing, International School of Materials Science and Engineering, Wuhan University of Technology, Wuhan 430070, P. R. China. E-mail: mlq518@whut.edu.cn; chenwei2005@whut.edu.cn

F. Lv, Dr. M. Luo, Prof. S. Guo

Department of Materials Science and Engineering, and BIC-ESAT, College of Engineering, Peking University, Beijing 100871, P. R. China. E-mail: guosj@pku.edu.cn

Dr. H. Zhu

School of Chemical and Material Engineering, Key Laboratory of Food Colloids and Biotechnology, Ministry of Education, Jiangnan University, Wuxi 214122, P. R. China.

[+] These authors contributed equally to this work and should be considered as co-first authors.

Experimental methods

Materials. Iron(II) phthalocyanine (FePc, 98%) was purchased from Shanghai D&B Biological Science and Technology Co., Ltd. (Shanghai, China). Titanium powders (99 wt.%, < 40 μm), aluminum powders (99 wt.%, < 40 μm) and graphite powders (99 wt.%, < 48 μm) were purchased from Alfa Aesar Chemical Co., Ltd. (Ward Hill, USA). Hydrogen fluoride (HF, 49%) was purchased from Aladdin Industrial Inc. (Shanghai, China). N, N-dimethylformamide (DMF, 99%) and potassium hydroxide (KOH, 95%) were purchased from Sinopharm Chemical Reagent Co., Ltd. (Shanghai, China). Pt/C powders (20 wt.%, < 3.5 nm) were purchased from Shanghai Hesen Electric Co., Ltd. (Shanghai, China).

Synthesis of Ti_3AlC_2. Ti_3AlC_2 was synthesized by following a reported method.[1] In details, titanium, aluminum and graphite powders were fully blended with a molar ratio of 3.0:1.5:2.0, ball-milled for 48 h, and cold-pressed into cylindrical discs under pressure of ~1 GPa. The discs were then placed in a tube furnace under flowing argon, and heated to 1400 °C for 2 h. After cooling to room temperature, the discs were milled to obtain the desired Ti_3AlC_2 powders.

Synthesis of $Ti_3C_2T_x$ MXenes. 0.2 g Ti_3AlC_2 powder was immersed into a 30 mL 49% HF solution. The mixture was stirred at room temperature for 48 h to obtain a homogeneous suspension. Let the suspension stand for 10 mi before collecting by centrifugation with a speed of 10 000 rpm. The resultant $Ti_3C_2T_x$ MXene was washed by deionized water and dried in vacuum at 60 °C for 12 h.

Synthesis of FePc/$Ti_3C_2T_x$ MXene. 30 mg of $Ti_3C_2T_x$ MXene and a certain amount of pure FePc powders were dispersed in DMF solution under ultrasonic condition for 1 h, respectively. Next, the FePc DMF solution was added to one containing $Ti_3C_2T_x$ MXene, followed by ultrasonic treatment for 0.5 h. The mixed solution was further stirred for 20 h to achieve the loading of FePc on $Ti_3C_2T_x$ MXenes. The FePc/$Ti_3C_2T_x$ MXene was collected by centrifugation, washed with DMF and ethanol, and dried in vacuum at 60 °C overnight.

Electrochemical measurements. All ORR measurements were conducted with a CHI 760D

electrochemical workstation (Chenhua, China) using a three-electrode cell at room temperature. A platinum (Pt) foil, a saturated calomel electrode (SCE) and a glassy carbon electrode (GCE) were used as counter, reference and working electrodes, respectively. The catalyst inks were prepared by primarily mixing 5 mg of catalyst powders and 5 mg of Vulcan XC72R carbon. Then the powder mixture was dispersed into a solution containing 800 μL of isopropanol, 150 μL of deionized water, and 50 μL of a 5 wt.% Nafion solution. After ultrasonic treatment for 1 h, the catalyst inks were drop-casted onto a polished GCE surface up to the catalyst loading amount of 0.25 mg_{cat} cm_{disk}^{-2}. An O_2-saturated 0.1 M KOH solution serving as electrolyte was continuously purged with O_2 in all ORR measurements. All the potentials were calibrated to a reversible hydrogen electrode (RHE) according to the equation, E(RHE) = E(SCE) + 0.0591pH + 0.24. Linear sweep voltammetry (LSV) was carried out with a rotating disk electrode (RDE) at different rotation rates of 400, 625, 900, 1 225, 1 600, and 2 025 rpm with a sweep rate of 5 mV s^{-1}. The collected LSV data can be analyzed to determine the ORR kinetics using the Koutecky–Levich equation:

$$\frac{1}{j} = \frac{1}{j_k} + \frac{1}{j_d} = -\frac{1}{nFAKC^o} - \frac{1}{0.62nFAD_{O_2}^{2/3}\upsilon^{-1/6}C^0\omega^{1/2}}$$

where j, j_k, and j_d stand for the measured, kinetic, and diffusion limiting currents, respectively, and n is the overall transferred electron number; F is the Faraday constant (96 500 cm^{-1}); A is the geometric electrode area (0.196 cm^2); K is the rate constant for oxygen reduction; C^o is the saturated concentration of oxygen in 0.1 $_M$ KOH (1.2 × 10^{-6} mol cm^{-1}); D_{O^2} is the diffusion coefficient of oxygen (1.87 × 10^{-6} cm^2 s^{-1}); υ is the kinetic viscosity of the solution (0.01013 cm^2 s^{-1}); and ω is the rotation rate (rad s^{-1}) of the electrode. Further, rotating ring-disk electrode (RRDE) measurements were conducted at 1 600 rpm to obtain the peroxide species (HO_2^-) yields and electron reduction number (n) as following the equation:

$$\mathrm{HO}_2^- = 200\frac{I_r/N}{I_d + I_r/N}$$

$$n = 4\frac{I_d}{I_d + I_r/N}$$

where I_d represents the disk current, I_r represents the ring current, and N represents the current collection efficiency (0.37) of the RRDE in our system. The turnover frequency (TOF) of catalytically active FeN_4 sites can be obtained according to the equation:

$$TOF = \frac{J_k N_e}{\omega_{Fe} C_{cat} N_A / M_{Fe}}$$

where J_k is the kinetic current density (A cm^{-2}), N_e is the electron number per Coulomb 6.24×10^{18}, ω_{Fe} is the active Fe content in catalysis, C_{cat} is the catalyst loading, N_A is the Avogadro constant (6.022×10^{23}), and M_{Fe} is the mass per mole of Fe (55.845 g mol^{-1}).

Characterizations. X-ray diffractometer (XRD) analysis was performed on a smart lab diffractometer (Rigaku, Japan) worked at 40 kV and 120 mA with a Co Kα radiation source (λ = 1.79 Å) in a 2θ angular range of 5−80°. Scanning electron microscope (SEM) images were collected using a JSM-7100F microscope (JEOL, Japan) at an acceleration voltage of 10 kV. Transmission electron microscope (TEM) images were divulged by a JEM-2100F/Titan G2 60-300 microscope (JEOL, Japan). Brunauer−Emmett−Teller (BET) tests were carried out using a TriStar-3020 gas adsorption analyzer at 77 K (Micromeritics Instrument Co., USA). Energy-dispersive X-ray spectrometer (EDS) mapping was conducted on an Oxford IE250 (Oxford Instruments, UK) system. Fourier transform infrared (FTIR) transmittance spectra were recorded using a Nicolet 6700 (Thermo Fisher Scientific Co., USA) IR spectrometer. Inductively coupled plasma mass spectrometry (ICP–MS) analysis was accomplished using a Thermo ICAP6300 equipment (Thermo Fisher Scientific Co., USA) to obtain the loading mass of FePc. X-ray photoelectron spectroscopy (XPS) were recorded on an ESCALAB 250 Xi spectrometer (VG Scientific Co., UK) with an Al Kα X-ray radiation (1486.6 eV). Ultraviolet photoemission spectroscopy (UPS) measurements were also carried out on an ESCA LAB 250 Xi spectrometer with He I resonance lines (21.2 eV). Ultraviolet−visible (UV−vis) absorption spectra

were recorded on a Lambda 35 spectrometer (Perkin–Elmer Instruments, USA). ^{57}Fe Mössbauer spectra were obtained using an Oxford MS-500 instrument (Oxford Instruments, UK) with a ^{57}Co source in a rhodium matrix at room temperature, and then were least squares fitted delivering the values of isomer shift (δ_{iso}), electric quadrupole splitting (ΔE_Q), and relative area of Fe ions. Temperature-dependent magnetic susceptibility plots were measured in the temperature range from 10 to 300 K with a physical property measurement system model 6000 (Quantum Design, USA). Electron spin resonance (ESR) spectra were recorded by an ER200-SRC-10/12 (Bruker, Germany) spectrometer at 300 K.

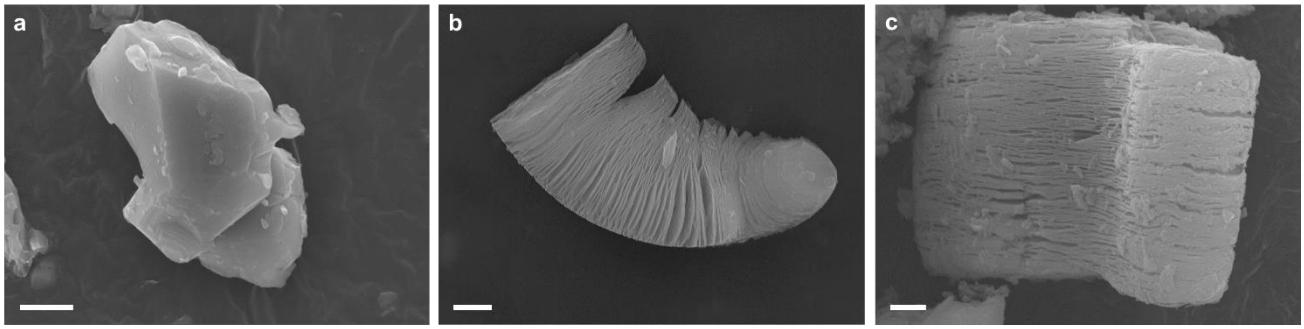

Figure S1. a–c) SEM images of pristine Ti_3AlC_2, $Ti_3C_2T_x$, and FePc/$Ti_3C_2T_x$, respectively. The scale bars are 1 μm.

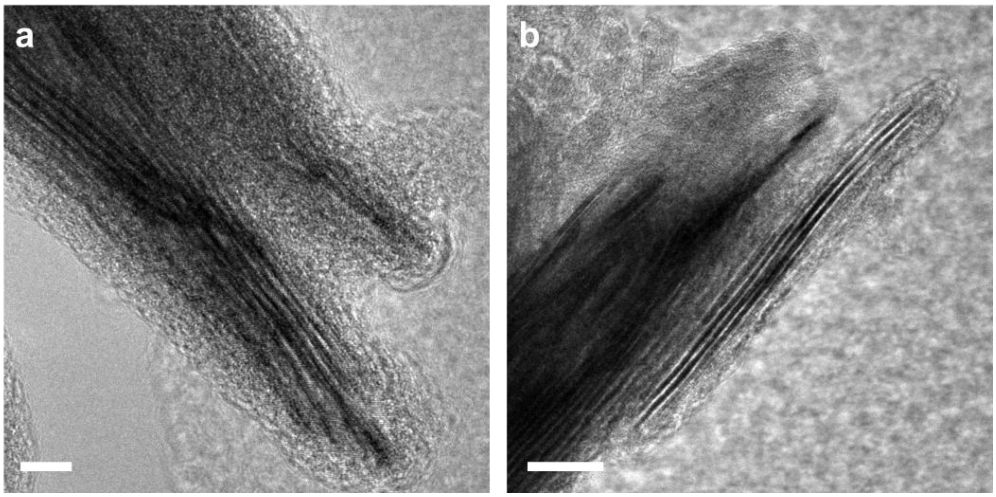

Figure S2. a, b) TEM images of FePc/$Ti_3C_2T_x$. The scale bars are 5 nm (a) and 10 nm (b).

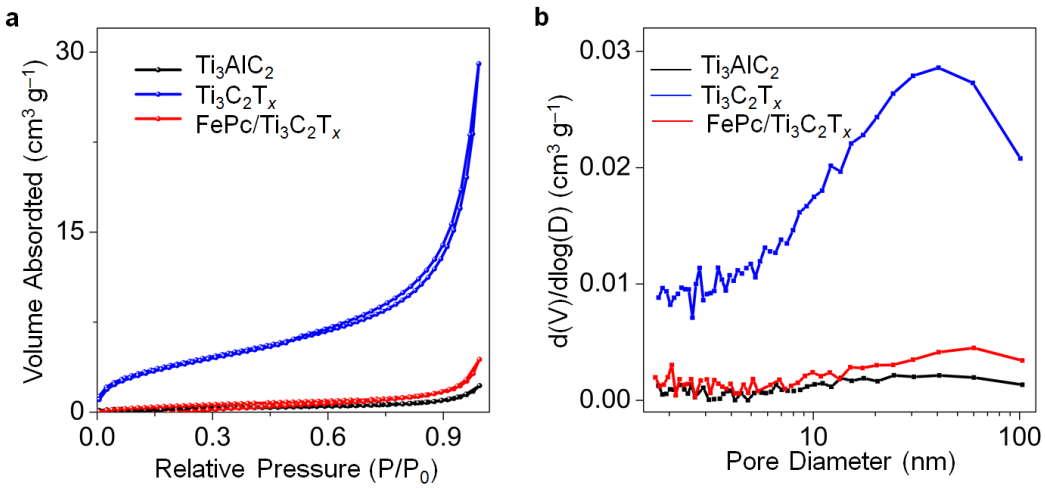

Figure S3. a) N_2 adsorption−desorption isotherms and b) pore-size distribution of Ti_3AlC_2, $Ti_3C_2T_x$, and FePc/$Ti_3C_2T_x$, repectively.

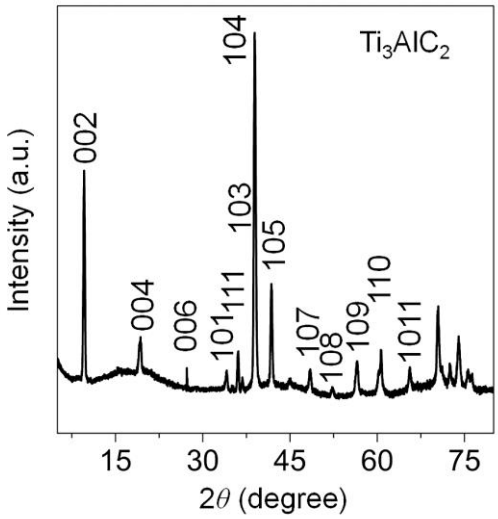

Figure S4. XRD pattern of Ti_3AlC_2.

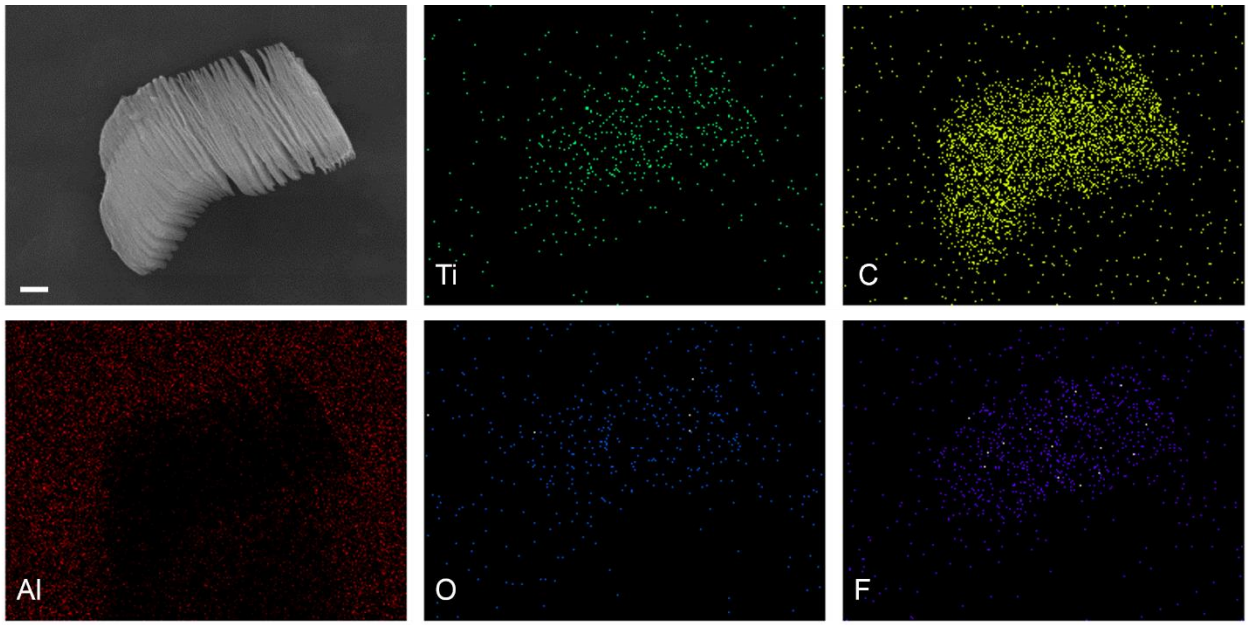

Figure S5. EDS mapping images of $Ti_3C_2T_x$. The scale bar is 1 μm.

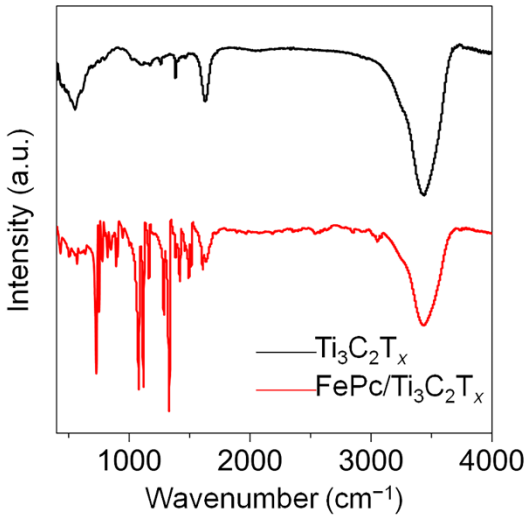

Figure S6. FTIR spectra of pristine $Ti_3C_2T_x$ and FePc.

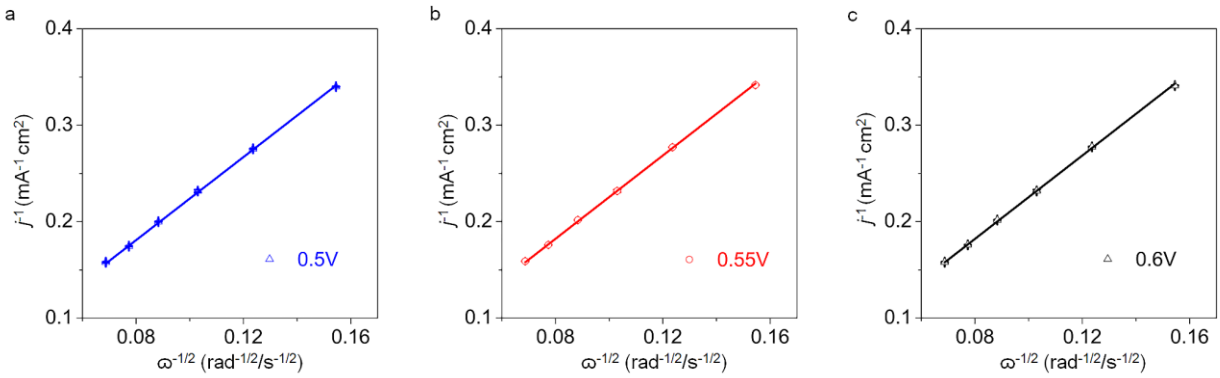

Figure S7. a–c) Koutecky–Levich plots of FePc/$Ti_3C_2T_x$ at 0.50, 0.55, and 0.60 V *vs*. RHE, respectively.

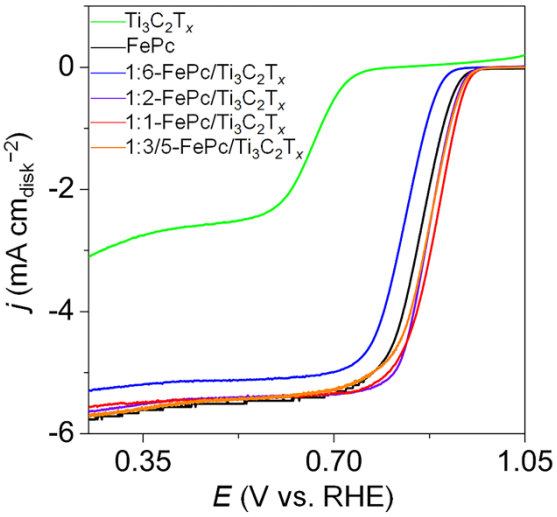

Figure S8. LSV curves of pristine FePc and FePc/$Ti_3C_2T_x$ with different weight ratios.

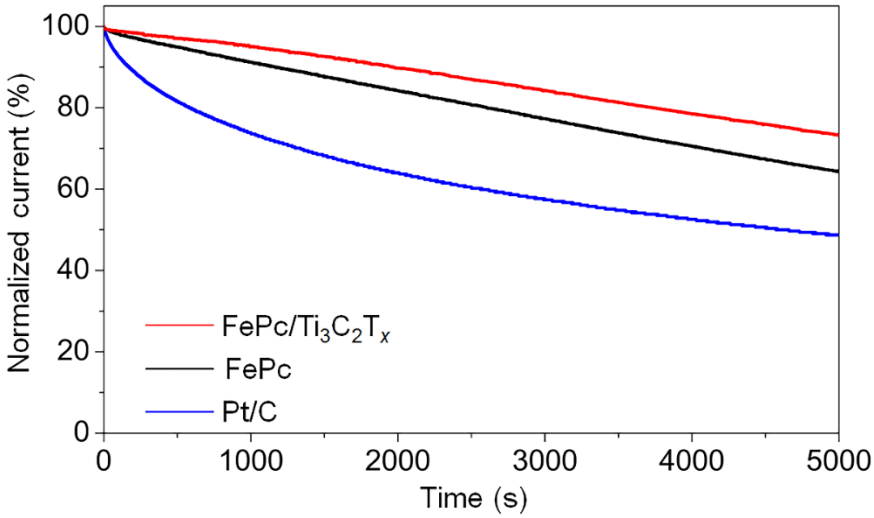

Figure S9. *i–t* curves of Pt/C, FePc and FePc/$Ti_3C_2T_x$ at 0.85 V *vs*. RHE.

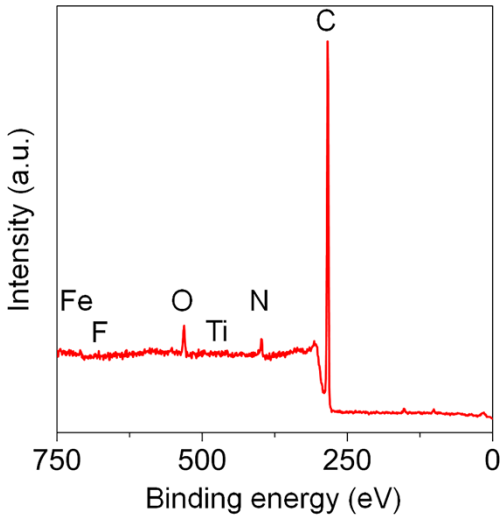

Figure S10. XPS survey spectrum of FePc/$Ti_3C_2T_x$.

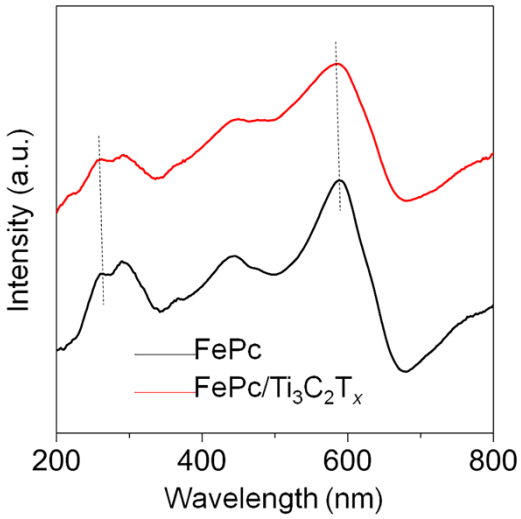

Figure S11. *UV–vis absorption spectra of pristine FePc and* FePc/$Ti_3C_2T_x$.

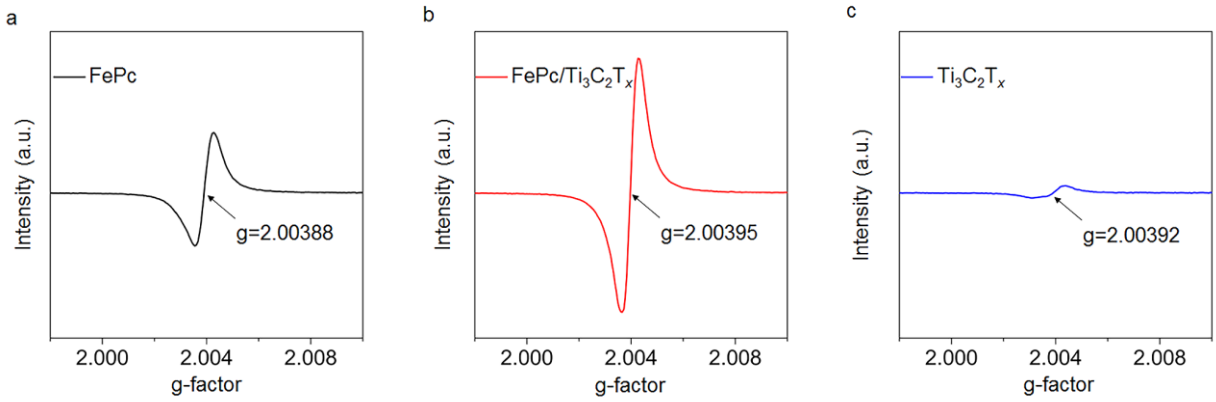

Figure S12. a–c) ESR spectra with g-factor of pristine FePc, FePc/$Ti_3C_2T_x$, and $Ti_3C_2T_x$.

Table S1. ICP−MS results of pristine FePc and FePc/$Ti_3C_2T_x$.

	Fe/wt.%	Ti/wt.%
FePc	9.17 ± 0.02	–
FePc/$Ti_3C_2T_x$	4.09 ± 0.02	29.94 ± 0.02

Table S2. Comparison of ORR performance between FePc/$Ti_3C_2T_x$ and state of the art Fe–N–C catalysts reported in the literatures.

Electrocatalysts	E_{onset}	$E_{1/2}$	J_k/mA cm^{-2}	Reference
FePc/$Ti_3C_2T_x$	0.97	0.89	3.0 at 0.9 V 15.5 at 0.85 V	This work
Fe-ISAs/CN	0.98	0.90	6.1 at 0.9 V 37.8 at 0.85 V	*Angew. Chem., Int. Ed.* **2017**, 56, 6937.[2]
pCNT@Fe@GL	0.97	0.87	2.1 at 0.9 V 9.7 at 0.85 V	*Adv. Mater.* **2017**, 29, 1606534.[3]
Fe–N–CNT–OPC	0.98	0.86	1.6 at 0.9 V 2.5 at 0.85 V	*Adv. Mater.* **2014**, 26, 6074.[4]
Fe/SNC	0.97	0.85	1.9 at 0.9 V 9.6 at 0.85 V	*Angew. Chem., Int. Ed.* **2017**, 56, 610.[5]
FePhen@MOF-$ArNH_3$	1.03	0.86	1.9 at 0.9 V 8.3 at 0.85 V	*Nat. Commun.* **2015**, 6. 7343.[6]
(DFTPP)Fe-Im-CNTs	1.1	0.92	13.3 at 0.9 V 35.8 at 0.85 V	*Angew. Chem., Int. Ed.* **2014**, 53, 6659.[7]
Fe@C-FeNC	0.98	0.89	5.2 at 0.9 V 17.3 at 0.85 V	*J. Am. Chem. Soc.* **2016**, 138, 3570.[8]
S,N-Fe/N/C-CNT	0.96	0.85	1.5 at 0.9 V 5.4 at 0.85 V	*Angew. Chem., Int. Ed.* **2017**, 56, 13800.[9]
Fe-N-CNFs	0.98	0.85	1.3 at 0.9 V 6.4 at 0.85 V	*Angew. Chem., Int. Ed.* **2015**, 54, 8179.[10]
Fe-NMCSs	1.02	0.86	1.7 at 0.9 V 6.9 at 0.85 V	*Adv. Mater.* **2016**, 28, 7948.[11]
Fe-N/C-800	0.97	0.82	0.56 at 0.9 V 2.4 at 0.85 V	*J. Am. Chem. Soc.* **2015**, 137, 5555.[12]

Fe2-Z8-C	0.98	0.87	2.6 at 0.9 V 12 at 0.85 V	*Angew. Chem., Int. Ed.* **2018**, 57, 1204.[13]
FePc–Py–CNTs	0.98	0.91	9.8 at 0.9 V 28.6 at 0.85 V	*Nat. Commun.* **2013**, 4, 2076.[14]

Table S3. Comparison of ORR performance between FePc/$Ti_3C_2T_x$ and other FePcs supported on different substrates reported in the literatures.

Electrocatalysts	E_{onset}	$E_{1/2}$	J_k/mA cm^{-2}	Reference
FePc/$Ti_3C_2T_x$	0.97	0.89	3.0 at 0.9 V 15.5 at 0.85 V	This work
FePc–Py–CNTs	0.98	0.91	9.8 at 0.9 V 28.6 at 0.85 V	*Nat. Commun.* 2013, 4, 2076.[14]
g-FePc	0.97	0.88	4.2 at 0.9 V 10.4 at 0.85 V	*ACS Catal.* 2013, 3, 1263.[15]
Pc-FePc/Mn-GCB	0.97	0.9	5 at 0.9 V 36 at 0.85 V	*Nano Energy* 2017, 34, 338.[16]
FePc-Cg	–	0.83	–	*J. Electroanal. Chem.* 1987, 221, 95.[17]

Table S4. ^{57}Fe *Mössbauer parameters and relative absorption area obtained for each component*

from the fitting of the experimental spectra. The isomer shift is given versus that of γ-Fe.

Sample	Component	A/%	δ_{iso}/mm s^{-1}	ΔE_Q/mm s^{-1}	Assignment
	Singlet	25.1	0.04	–	γ-Fe
FePc	D1	–	–	–	High-spin Fe(II)
	D2	74.9	0.239	2.673	Intermediate-spin Fe(II)
	Singlet	10	0	–	γ-Fe
FePc/$Ti_3C_2T_x$	D1	47	0.245	0.483	High-spin Fe(II)
	D2	42.6	0.189	2.723	Intermediate-spin Fe(II)

References

[1] Q. Peng, J. Guo, Q. Zhang, J. Xiang, B. Liu, A. Zhou, R. Liu, Y. Tian, *J. Am. Chem. Soc.* **2014**, 136, 4113.

[2] Y. J. Chen, S. F. Ji, Y. G. Wang, J. C. Dong, W. X. Chen, Z. Li, R. A. Shen, L. R. Zheng, Z. B. Zhuang, D. S. Wang, Y. D. Li, *Angew. Chem., Int. Ed.* **2017**, 56, 6937.

[3] S. H. Ahn, X. Yu, A. Manthiram, *Adv. Mater.* **2017**, 29, 1606534.

[4] J. Liang, R. F. Zhou, X. M. Chen, Y. H. Tang, S. Z. Qiao, *Adv. Mater.* **2014**, 26, 6074.

[5] P. Z. Chen, T. P. Zhou, L. L. Xing, K. Xu, Y. Tong, H. Xie, L. D. Zhang, W. S. Yan, W. S. Chu, C. Z. Wu, Y. Xie, *Angew. Chem., Int. Ed.* **2017**, 56, 610.

[6] K. Strickland, M. W. Elise, Q. Y. Jia, U. Tylus, N. Ramaswamy, W. T. Liang, M. T. Sougrati, F. Jaouen, S. Mukerjee, *Nat. Commun.* **2015**, 6, 7343.

[7] P. J. Wei, G. Q. Yu, Y. Naruta, J. G. Liu, *Angew. Chem., Int. Ed.* **20**14, 53, 6659.

[8] W.-J. Jiang, L. Gu, L. Li, Y. Zhang, X. Zhang, L.-J. Zhang, J.-Q. Wang, J.-S. Hu, Z. Wei, L.-J. Wan, *J. Am. Chem. Soc.* **2016**, 138, 3570.

[9] H. J. Shen, E. Gracia-Espino, J. Y. Ma, K. T. Zang, J. Luo, L. Wang, S. S. Gao, X. Mamat, G. Z. Hu, T. Wagberg, S. J. Guo, *Angew. Chem., Int. Ed.* **2017**, 56, 13800.

[10] Z.-Y. Wu, X.-X. Xu, B.-C. Hu, H.-W. Liang, Y. Lin, L.-F. Chen, S.-H. Yu, *Angew. Chem., Int. Ed.* **2015**, 54, 8179.

[11] F. L. Meng, Z. L. Wang, H. X. Zhong, J. Wang, J. M. Yan, X. B. Zhang, *Adv. Mater.* **2016**, 28, 7948.

[12] W. Niu, L. Li, X. Liu, N. Wang, J. Liu, W. Zhou, Z. Tang, S. Chen, *J. Am. Chem. Soc.* **2015**, 137, 5555.

[13] Q. T. Liu, X. F. Liu, L. R. Zheng, J. L. Shui, *Angew. Chem., Int. Ed.* **2018**, 57, 1204.

[14] R. Cao, R. Thapa, H. Kim, X. Xu, K. M. Gyu, Q. Li, N. Park, M. Liu, J. Cho, *Nat. Commun.* **2014**, 4, 2076.

[15] Y. Jiang, Y. Lu, X. Lv, D. Han, Q. Zhang, L. Niu, W. Chen, *Acs Catal.* **2013**, 3, 1263.

[16] Z. Zhang, M. Dou, J. Ji, F. Wang, *Nano Energy* **2017**, 34, 338.

[17] A. V. D. Putten, A. Elzing, W. Visscher, E. Barendrecht, *J. Electroanal. Chem.* **1987**, 221, 95.